Heliyon 9 (2023) e16318

Contents lists available at ScienceDirect

Heliyon

journal homepage: www.cell.com/heliyon

Research article

A ubiquitination-mediated degradation system to target 14-3-3-binding phosphoproteins

Zhaokai Li [a,b], Xiaoqiang Huang [c], Mohan Li [d], Y. Eugene Chen [a,c,e], Zhong Wang [a,*], Liu Liu [a,**]

[a] Department of Cardiac Surgery, Cardiovascular Center, University of Michigan, Ann Arbor, MI 48109, USA
[b] Department of Emergency Medicine, China-Japan Friendship Hospital, Beijing 100029, China
[c] Center for Advanced Models for Translational Sciences and Therapeutics, Department of Internal Medicine, University of Michigan, Ann Arbor, MI 48109, USA
[d] Department of Geriatrics, Chinese Academy of Medical Sciences, Peking Union Medical College Hospital, Beijing 100730, China
[e] Department of Internal Medicine, Cardiovascular Center, University of Michigan, Ann Arbor, MI 48109, USA

ARTICLE INFO

Keywords:
Targeted protein degradation
von hippel-lindau
14-3-3
Phosphorylation
Ubiquitination

ABSTRACT

The phosphorylation of 14-3-3 binding motif is involved in many cellular processes. A strategy that enables targeted degradation of 14-3-3-binding phosphoproteins (14-3-3-BPPs) for studying their functions is highly desirable for basic research. Here, we report a phosphorylation-induced, ubiquitin-proteasome-system-mediated targeted protein degradation (TPD) strategy that allows specific degradation of 14-3-3-BPPs. Specifically, by ligating a modified von Hippel-Lindau E3-ligase with an engineered 14-3-3 bait, we generated a protein chimera referred to as Targeted Degradation of 14-3-3-binding PhosphoProtein (TDPP). TDPP can serve as a universal degrader for 14-3-3-BPPs based on the specific recognition of the phosphorylation in 14-3-3 binding motifs. TDPP shows high efficiency and specificity to a difopein-EGFP reporter, general and specific 14-3-3-BPPs. TDPP can also be applied for the validation of 14-3-3-BPPs. These results strongly support TDPP as a powerful tool for 14-3-3 related research.

1. Introduction

Controlling a protein's concentration level is key to studying its function. Strategies that specifically target and degrade a protein of interest (POI) have emerged in recent years, which are collectively called targeted protein degradation (TPD) [1]. Among them, strategies based on the ubiquitin-proteasome system (UPS), a crucial protein degradation system in eukaryotic cells [2,3], including heterobifunctional small molecules like proteolysis targeting chimeras (PROTACs) [4], protein/peptide-based degraders like affinity-directed protein missiles (AdPROMs) [5], molecular glue [6], dTAG [7], etc., show great efficiency for protein degradation.

However, current TPD strategies still have their limitations. Only a few tag-based TPD strategies [7–9] (reviewed by Burslem, et al. [10]) have been developed to target proteins with post-translational modifications (PTMs), while specific TPD strategies are still lacking for major types of PTMs that widely exist in eukaryotic cells, including protein phosphorylation, methylation, acetylation, etc., which play an important role in regulating protein functions. The same protein under different PTM statuses can display different

* Corresponding author.
** Corresponding author.
E-mail addresses: zhongw@med.umich.edu (Z. Wang), luvul@med.umich.edu (L. Liu).

https://doi.org/10.1016/j.heliyon.2023.e16318
Received 11 December 2022; Received in revised form 8 May 2023; Accepted 12 May 2023
Available online 20 May 2023

functions. Therefore, the development of PTM-specific degradation systems is desirable.

The TPD strategy has the potential to regulate specific kinds of phosphorylated proteins. While at least three quarters of the proteome is phosphorylated [11], protein phosphorylation exists in every organism and participates in most biological events [12]. The phosphorylation/dephosphorylation states of proteins can be distinguished by their "readers" that interact with the binding motifs. 14-3-3 is one of those phosphorylation readers. As one of the most expressed proteins in eukaryotic cells [13], 14-3-3 is a highly conserved protein family consisting of 7 isoforms (i.e., β, γ, ε, ζ, η, τ, and σ) [14]. The function of 14-3-3 largely depends on its interaction with phospho-serine/threonine (phospho-S/T) in phosphoproteins [15], which are embedded within phospho-14-3-3 binding motifs.

Here we describe a new TPD system, namely TDPP, for Targeted Degradation of Phospho-14-3-3-binding-motif-embedded (P-14-3-3-BME) Protein. TDPP is a protein chimera made by coupling a modified von Hippel-Lindau (VHL) E3-ligase [16] with an engineered 14-3-3ζ bait. Independent experiments showed that TDPP targets 14-3-3-BPPs with high affinity and efficiency. Furthermore, with high specificity to target the proteins of interest, it will likely be a powerful biological tool for protein-protein interaction (PPI) research, regulation of the phosphorylation/dephosphorylation status of multiple proteins and the level of phospho-proteins at the whole-cell level.

2. Results

2.1. Design of a degradation system targeting 14-3-3-BPPs

Inspired by previously described hetero bifunctional degrader strategies [10,17–20], we developed a degradation system that specifically targets 14-3-3-BPPs. Following the logic that a 14-3-3 bait is appropriate to recruit the 14-3-3-BPP targets and an E3 ligase

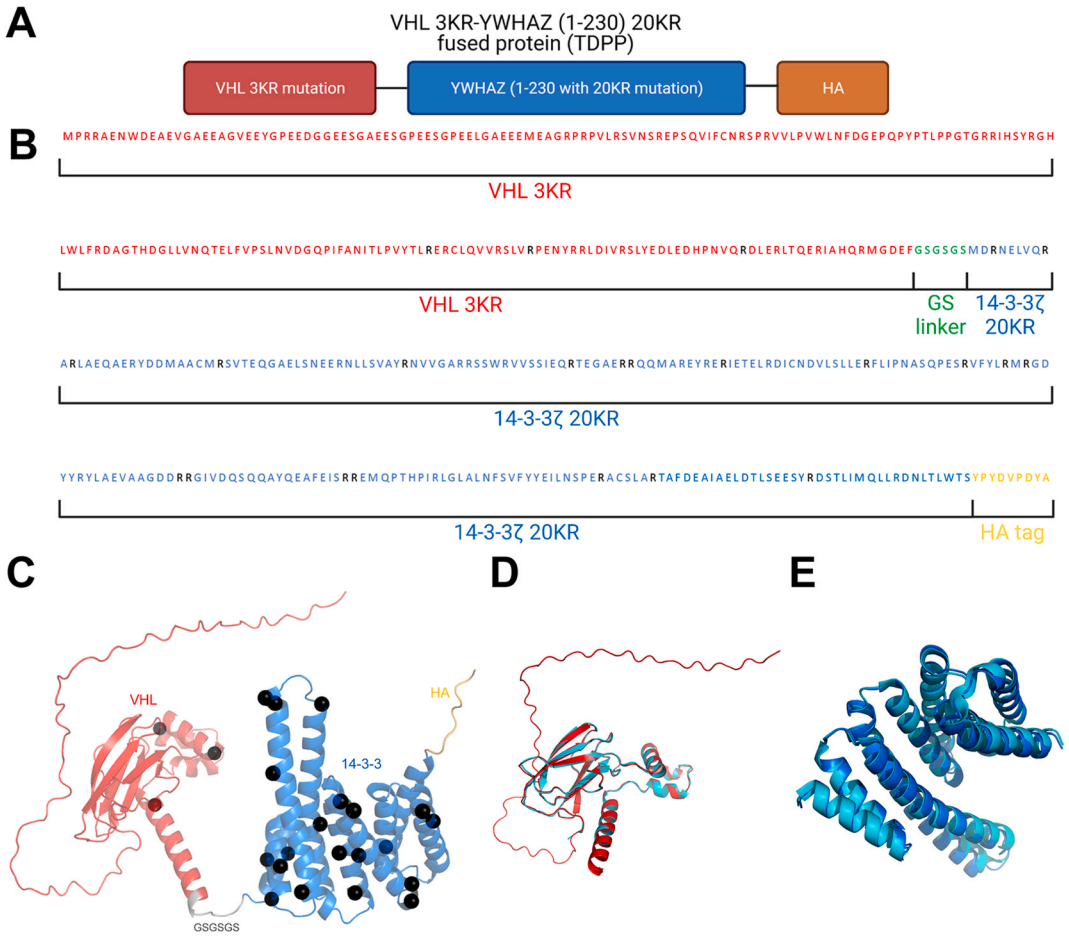

Fig. 1. Illustration and de novo structure modeling of a degrader of 14-3-3-BPPs. A. TDPP fused protein design. B. Sequence partition information of TDPP. C. Full-length structure model generated by ColabFold [26]. KR mutation sites are highlighted in black spheres. D. Comparison of predicted VHL 3 KR model and experimental VHL structure. Red: predicted VHL (extracted from full-length model); cyan: experimental VHL structure (PDB ID: 4WQO). E. Comparison of predicted 14-3-3ζ 20 KR model and experimental 14-3-3ζ structure. Blue: predicted 14-3-3ζ (extracted from full-length model); cyan: experimental 14-3-3ζ structure (PDB ID: 2O02). See also Fig. S1.

is necessary to introduce the POI to UPS for degradation, an E3-14-3-3 ligated protein became the fundamental structure of the degrader described here. While VHL is an E3 ligase that numerous TPD strategies were based on [16,21], and 14-3-3ζ ranks as one of the major 14-3-3 isoforms in humans [13], those two were picked as the UPS-binding part and the POI-binding part, respectively. It

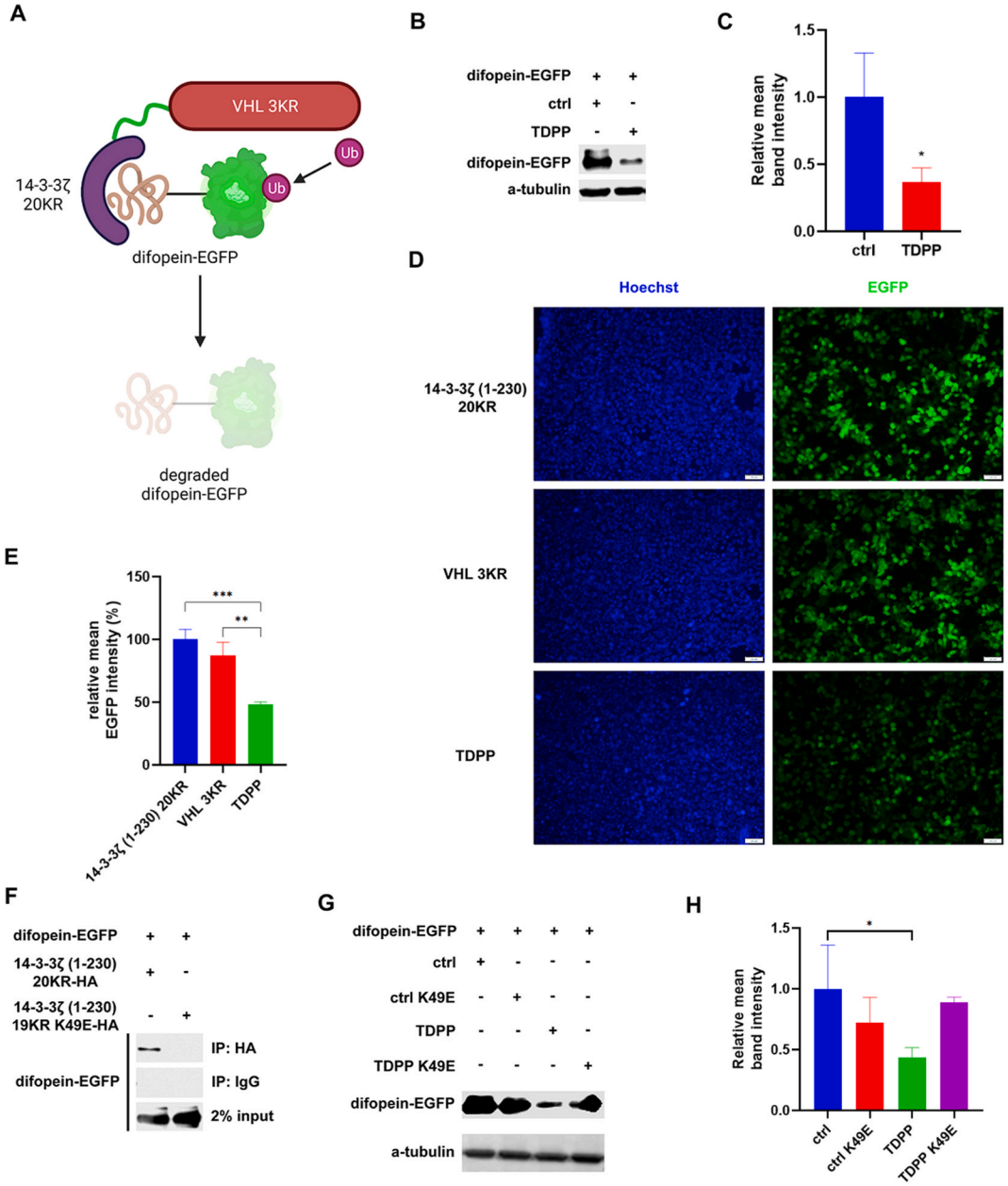

Fig. 2. TDPP degrades difopein-EGFP. A. Working model of TDPP-induced degradation of difopein-EGFP. Undegraded difopein-EGFP protein chimera has a green fluorescent ability from the EGFP tag. Since the 14-3-3 bait in TDPP could specifically interact with the difopein tag in difopein-EGFP, TDPP will provide the proximity of UPS to difopein-EGFP and degrade it, in which condition the green fluorescent intensity will decrease. B, C. Western blot result (B) and quantification of band intensity (C) of difopein-EGFP in HEK293T/17 cells co-transfected with expression plasmids of 14-3-3ζ (1–230) 20 KR-HA (referred as ctrl) or VHL 3 KR-14-3-3ζ (1–230) 20 KR-HA (referred as TDPP). D, E. Fluorescence assay result (D) and fluorescence intensity quantification (E) of HEK293T/17 cells transfected with difopein-EGFP vector, along with control vectors (14-3-3ζ (1–230) 20 KR or VHL 3 KR) or TDPP vector. F. Immunoprecipitation result of interaction between 14-3-3ζ (1–230) 20 KR-HA/14-3-3ζ (1–230) 19 KR K49E-HA and difopein-EGFP. IP: 14-3-3ζ (1–230) 20 KR-HA/14-3-3ζ (1–230) 19 KR K49E-HA. IB: difopein-EGFP. G, H. Western blot result (G) and quantification of band intensity (H) of difopein-EGFP in HEK293T/17 cells co-transfected with expression plasmids of 14-3-3ζ (1–230) 20 KR-HA (referred as ctrl), 14-3-3ζ (1–230) 19 KR K49E-HA (referred as ctrl K49E), VHL 3 KR-14-3-3ζ (1–230) 20 KR-HA (referred as TDPP), or VHL 3 KR-14-3-3ζ (1–230) 19 KR K49E-HA (referred as TDPP K49E). Data are represented as mean ± SEM.

was reported that the C-terminal of wildtype (WT) 14-3-3 protein isoforms decrease their binding efficiency to 14-3-3 binding motif [22–24], so a C-terminal truncated version of 14-3-3ζ was used, i.e., 14-3-3ζ was truncated to 14-3-3ζ (1–230). Finally, giving to the protein nature of the protein chimera described above, which would potentially lead to auto-ubiquitination and auto-degradation when it is exposed to UPS, all the lysine (K) residues within the protein chimera were mutated to arginine (R) to avoid such a side-effect following a proven strategy [25], and VHL 3 KR-14-3-3ζ (1–230) 20 KR (referred to as TDPP, Fig. 1, A and B) was finally developed and evaluated here after.

A protein's structure determines its function. To know if the domains of the protein chimera [i.e., VHL 3 KR and 14-3-3ζ (1–230) 20 KR] in TDPP could properly fold into desired structures, we used ColabFold [26] which is adapted from AlphaFold2 [27] to perform de novo structure prediction of TDPP without any structure templates. Specifically, we directly submitted the TDPP protein sequence to the Colab Fold server (see STAR Methods) and chose to predict five models with AMBER refinement. All other parameters were used as default. The average predicted local-distance difference test (pLDDT) scores for all five models range from 81.2 to 82.7 (Fig. S1B), indicating the overall high quality of the models [usually an LDDT score of 0.6 or greater is considered a reasonable model and scores above 0.8 are great models [28]]. The relatively low per-residue LDDT scores suggest that the N-terminal of VHL, the GSGSGS linker, and the hemagglutinin (HA) tag regions are of lower quality (Fig. S1A), consistent with the annotation in UniProt that the N-terminal (i.e., amino acids 1–65) of VHL is disordered. Otherwise, the other regions of VHL and 14-3-3ζ are well folded (Fig. S1C). Except the second-ranking model (i.e., *rank_2*), the other four models have their N-terminal tail inserted into the binding groove of 14-3-3ζ (Fig. S1C). However, no evidence supports the binding between the N-terminal of VHL and 14-3-3ζ and the insertions are possibly caused by the less accurate modeling of the VHL N-terminus. Fig. 1C depicts the overall structure of TDPP (*rank_2* is used). As shown in Fig. 1, D and E, the predicted VHL and 14-3-3 protein components match perfectly with their native counterparts respectively, except for the disordered region. Taken together, de novo structure modeling suggests that the individual components of TDPP can fold properly to perform desired function.

2.2. TDPP degrades difopein-EGFP

The fundamental hypothesis of TDPP as a TPD strategy is that TDPP could interact with 14-3-3-BPPs when they are phosphorylated, and their interaction with TDPP could lead to the degradation of the interacting proteins themselves. Because of the technical difficulty to control the dynamic change of the phosphorylation/dephosphorylation status of 14-3-3-BPPs in cells, the process to evaluate TDPP's efficiency was divided into two separate parts: whether TDPP could induce the degradation of its interacting partners and whether TDPP could induce the degradation of 14-3-3-BPPs. The former question was assessed with a phosphorylation-independent evaluation system. A small peptide inhibitor of 14-3-3 protein, difopein [29,30], was fused to an EGFP fluorescence reporter. Such a difopein-EGFP fused protein could become an excellent POI of TDPP strategy, which mimics the binding of 14-3-3-BME proteins to 14-3-3 and holds a reliable interaction ability with the TDPP chimera, all while the interaction is phosphorylation-independent [30]. Thus, the 14-3-3-difopein interaction was expected to induce stable difopein-EGFP degradation and therefore lead to declining EGFP fluorescence (Fig. 2A). Both the TDPP chimera and difopein-EGFP fused protein were expressed in HEK293T/17 cells using the co-transfection strategy (see Methods for details). As predicted, we observed a significantly decreased EGFP protein level when TDPP was introduced, compared with the control group (Fig. 2, B and C). In parallel, we also observed a significant decrease in EGFP fluorescence for the TDPP-treated group (Fig. 2, D and E).

We next determined whether the decreased difopein-EGFP phenotype was caused by its interaction with TDPP. Since lysine 49 (K49) residue of 14-3-3 plays a key role in interacting with difopein or 14-3-3-BPPs [31–33], a 14-3-3ζ K49E mutant is predicted to diminish the interaction. Because the previously reported TPD systems have a high turnover rate [7,34,35], we reasonably speculated that each individual difopein-EGFP protein that interacts with TDPP will also be transiently degraded and impossible to detect by co-immunoprecipitation (co-IP). Thus, instead of using a whole TDPP, we used only the bait part of TDPP, 14-3-3ζ (1–230) 20 KR-HA, to evaluate its interaction with difopein-EGFP, along with the K49E mutant, 14-3-3ζ (1–230) 19 KR K49E-HA, as the control. While although K49 has been mutated to R in the 14-3-3ζ (1–230) 20 KR-HA construct, the interaction of 14-3-3ζ (1–230) 20 KR-HA with difopein-EGFP can be detected by immunoprecipitation, meanwhile K49E mutation abolishes the interaction of 14-3-3ζ (1–230) 20 KR-HA with difopein-EGFP (Fig. 2F). Also, as expected, the single K49E mutation also significantly diminished the degradation efficiency (Fig. 2, G and H), indicating an interaction-dependent degradation of difopein-EGFP by TDPP.

2.3. TDPP degrades 14-3-3-BPPs

Beyond the evaluator protein difopein-EGFP, 14-3-3-BPPs are the major POIs of TDPP. To assess the influence TDPP has on the general 14-3-3-BPPs, the overall phospho-(Ser)-14-3-3-binding-motif level of HEK293T/17 cells was measured with its specific antibody, which was selected to reflect the general 14-3-3-BPPs level, and TDPP was again expressed in cells by transfection. During the evaluation, okadaic acid (OA), an inhibitor for PP2a and a partial inhibitor for PP1 [36], was also used to enhance the total phosphorylation level. As expected, the overall phospho-(Ser)-14-3-3-binding-motif level in cells decreases by introducing TDPP (Fig. 3, A–C). The decrease can be observed under both normal conditions (Fig. 3A, lane 1 vs. 3, and Fig. 3B, upper panel) and dephosphorylation-inhibited treatment (Fig. 3A, lane 2 vs. 4, and Fig. 3B, lower panel), although exceptions still exist. Overall, these data show that TDPP can efficiently degrade 14-3-3-BPPs under both normal and high-phosphorylation conditions.

To determine if TDPP's degradation efficiency varies among different phosphoproteins, four 14-3-3-BPPs with well-established phosphorylation-dependent 14-3-3-interacting mechanisms, were selected for further evaluation. Among those proteins, histone deacetylase 4 (HDAC4) is a member of class IIa HDACs that plays an important role in tissue-specific growth and development [37].

Histone deacetylase 5 (HDAC5) is another gene transcription repressor that regulates myogenesis [38], cell proliferation [39] and other processes. Forkhead Box O1 (FoxO1) is a transcription factor that involves in metabolic homeostasis [40], and Cofilin 1 (CFL1) is an F-actin severing protein functioning in cytoskeletal homeostasis [41,42]. During the evaluation, among those four proteins, three showed significantly decreased protein levels by introducing TDPP (Fig. 3, D and E), while no significant difference was observed for CFL1 (Fig. S2, A and B). We reasoned this variance may be due to the different 14-3-3-interaction ability and different subcellular distribution.

We next determined if the observed degradation is phosphorylation-dependent. Among the four 14-3-3-BPPs evaluated above, HDAC4 is one that contains three known 14-3-3-binding motifs [43–47], which enables higher possibility to be phosphorylation-dependently degraded by TDPP in theory, so it was selected as a known 14-3-3-BPP for further evaluation. The phospho-HDAC4 (pHDAC4)-14-3-3 interaction has been well-established [48]. HDAC4 phospho-S632 (pS632), which bears a P-14-3-3 binding motif, is a portion of HDAC4 that could phosphorylation-dependently interacted with 14-3-3. With an antibody that specifically detects HDAC4 pS632, we observed that TDPP can target HDAC4 pS632 (Fig. 3, F and G), consolidating a phosphorylation-induced degradation mechanism of TDPP. Taken together, these data established a phosphorylation-dependent degradation of 14-3-3-BPPs induced by TDPP.

2.4. TDPP validates BICRA as a new 14-3-3 interaction target protein

Another application of TDPP is to validate potential 14-3-3-BPPs. We have previously worked on the SWI/SNF complex [49–53] that is involved in 14-3-3-related pathways [54]. We thus applied TDPP to determine the potential agent that mediates

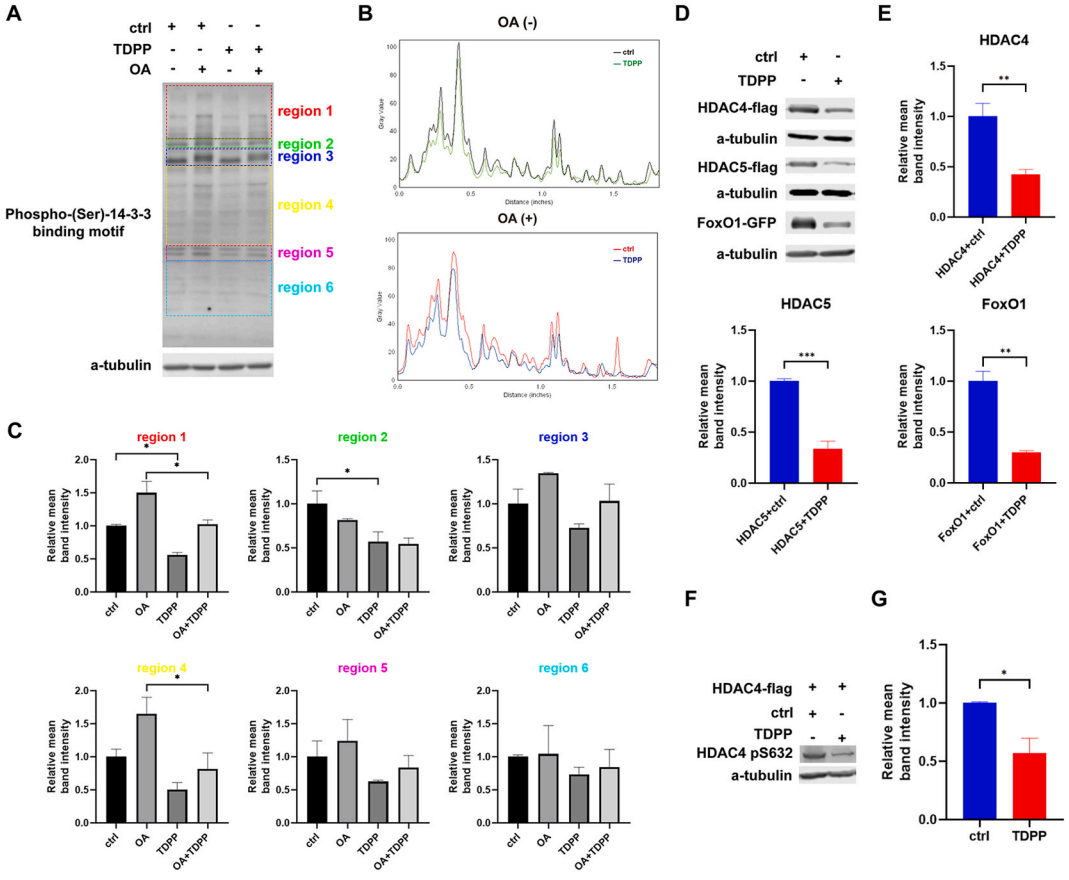

Fig. 3. TDPP degrades 14-3-3-BPPs. A. Western blot of phospho-(Ser)-14-3-3-binding-motif treated with control/TDPP vector with/without 10 nM OA. Different molecular weight ranges were grouped as different regions and marked as different colors, which were roughly grouped by similar band intensity and reflect the difference among treatments. The grey value of bands and regions were quantified and further analyzed in panel B and C, respectively. B. Illustration of the grey value distribution of phospho-(Ser)-14-3-3-binding-motif in each treatment in panel A. X axis represents the distance to the top edge of the blot results. Upper panel: lane 1 (black) vs. lane 3 (green). Lower panel: lane 2 (red) vs. lane 4 (blue). C. Quantification of phospho-(Ser)-14-3-3-binding-motifembedded proteins with different molecular weight in panel A. D and E. Western blot results (D) and the quantifications (E) of several different phospho-14-3-3-binding-motif embedded proteins (HDAC4, HDAC5, FoxO1) in HEK293T/17 cells treated with control/TDPP vectors. F and G. Western blot result (F) and the quantification (G) of HDAC4 phospho-S632 in a HDAC4 wildtype vectors transfected HEK293T/17 cells treated with control/TDPP vector. Data are represented as mean ± SEM. See also Fig. S2.

14-3-3-SWI/SNF interaction. Using 14-3-3-Pred [55], we identified BICRA [56] as a potential P-14-3-3-BME subunit of the SWI/SNF complex; the S801, S805, S815, S866, and S1477 residues in BICRA were predicted as potential 14-3-3-binding sites. The protein level of BICRA decreased substantially with the introduction of TDPP (Fig. 4, A and B), supporting BICRA as a P-14-3-3-BME subunit. This experiment suggests TDPP as a useful tool for validating potential 14-3-3 targeting proteins.

3. Discussion

In this study, we report for the first time a phosphorylation-induced TPD strategy, TDPP, which specifically degrades 14-3-3-BPPs by ligating an engineered 14-3-3ζ protein to a modified VHL E3-ligase. TDPP is a TPD system just like most of the previously reported strategies like PROTACs. Fundamentally by utilizing the native UPS that including several ubiquitin ligases and the proteosome, TDPP enables a specific recognition, interaction and degradation of our POIs based on the binding affinity of 14-3-3 bait to them. As a protein chimera, TDPP provides the POI preys the proximity to E3 ligases and introduce them to the UPS, thus a targeted protein degradation is achieved. Based on our results, as designed, the TDPP protein chimera can efficiently bind and present 14-3-3-BPPs to E3-ligase which then introduces the targeted 14-3-3-BPPs to UPS for degradation (Fig. 5).

Several innovations were applied in the design of TDPP's protein structure. The most important one is the KR mutation to block the auto-ubiquitination and auto-degradation, which is predictable because of the protein nature of TDPP. One concern about the modification is that K49 is the key phosphoprotein-binding residue [31,57,58], by which the KR mutation may impair the interaction ability of TDPP with the POIs in this study. However, on one hand, it is also reported that multiple KR mutations in 14-3-3 could lead to a much more complex consequence to its interaction ability with 14-3-3-BPPs [59], which may counteract or reverse the undesirable effect of K49R mutation. On the other hand, arginine residue holds positive charge, just like the lysine residue, which represents that the KR mutation is almost like a synonymous substitution. Glutamic acid residue, on the opposite, holds negative charge, thus KE mutation could totally disrupt the core interaction ability of the mutated protein with its binding partners. In this study, the *in silico* prediction (Fig. 1, C–E) showed TDPP reserves the interaction ability with 14-3-3-BPPs, and the *in vivo* results (Fig. 2F) showed that significant interactions still exist between TDPP and our POIs.

The high efficiency of TDPP has been confirmed by a diversity of evaluators. Compared with 14-3-3-BPPs, the stable difopein-EGFP reporter, which does not have a phosphorylation/dephosphorylation switch and which has a much-limited interaction with other unspecified proteins in cells, is appropriate for examining TDPP's degradation efficiency (Fig. 2A). As expected, significant degradation of difopein-EGFP by TDPP was observed (Fig. 2, B–E) and, in contrast, the TDPP K49E significantly abolished degradation efficiency (Fig. 2, G and H), strongly indicating that TDPP is an interaction-based degradation system that specifically targets 14-3-3-binding proteins.

TDPP displays an overall high efficiency in degrading 14-3-3-BPPs (Fig. 3), though some variance in degradation efficiency was observed for different phosphoproteins. This is understandable because a few factors including the phosphorylation percentage of 14-3-3-BPPs, the half-life time, the spatiotemporal distribution, and the ability to bind 14-3-3 can all impact the apparent degradation efficiency. For instance, the binding affinity to 14-3-3 can have more than a 1000-fold span among different 14-3-3-BPPs [60]. It is reasonable that TDPP may fail to degrade some proteins even if they bear a phsopho-14-3-3 binding motif, in which case TDPP could be locally saturated by POIs with relatively high binding affinity, while the low binding affinity targets could not be efficiently degraded.

Unlike that most of the previously reported TPD systems were designed for the degradation of one specific POI respectively, TDPP was designed to degrade the 14-3-3-BPPs, which are multiple proteins grouped together by a structure similarity and the ability to interact with 14-3-3 while phosphorylated. Thus, according to the nature of TDPP-induced degradation, "motif of interest (MOI)" or "PTM of interest (PTMOI)" will be better than the widely used "protein of interest" concept to describe the targets of TDPP, i.e., the "single" target of TDPP is P-14-3-3 binding motif. While 14-3-3-BPPs are mostly within the 14-3-3 interactome, such a strategy could be significant to investigate the 14-3-3-BPPs. The 14-3-3-BPPs are a group of proteins defined by a specific sequence within their protein structure. Though bearing special features, the 14-3-3-BPPs are not fully defined. It is challenging to determine the 14-3-3 binding motif with traditional methods like co-IP. Although computational tools have been developed to predict 14-3-3 interacting sites, a precise method to validate the predicted results is missing. Since TDPP specifically targets 14-3-3-BPPs, we believe that it will be a useful tool for validating potential 14-3-3-BPPs including BICRA studied here. Furthermore, TDPP can potentially target SARS-CoV-2, as it is reported that SARS-CoV-2 nucleocapsid protein is recognized by 14-3-3 [61].

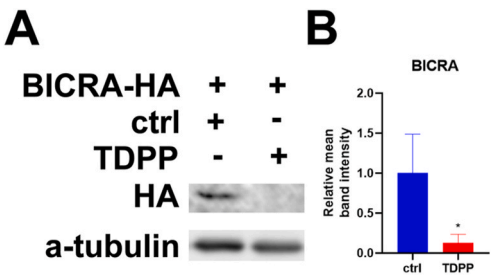

Fig. 4. TDPP validates BICRA as a new 14-3-3 interaction target protein. A. Western blot of BICRA-HA level in its expression HEK293T/17 cells transfected with control/TDPP vectors. B. Relative mean band intensity of BICRA-HA Western blot. Data are represented as mean ± SEM.

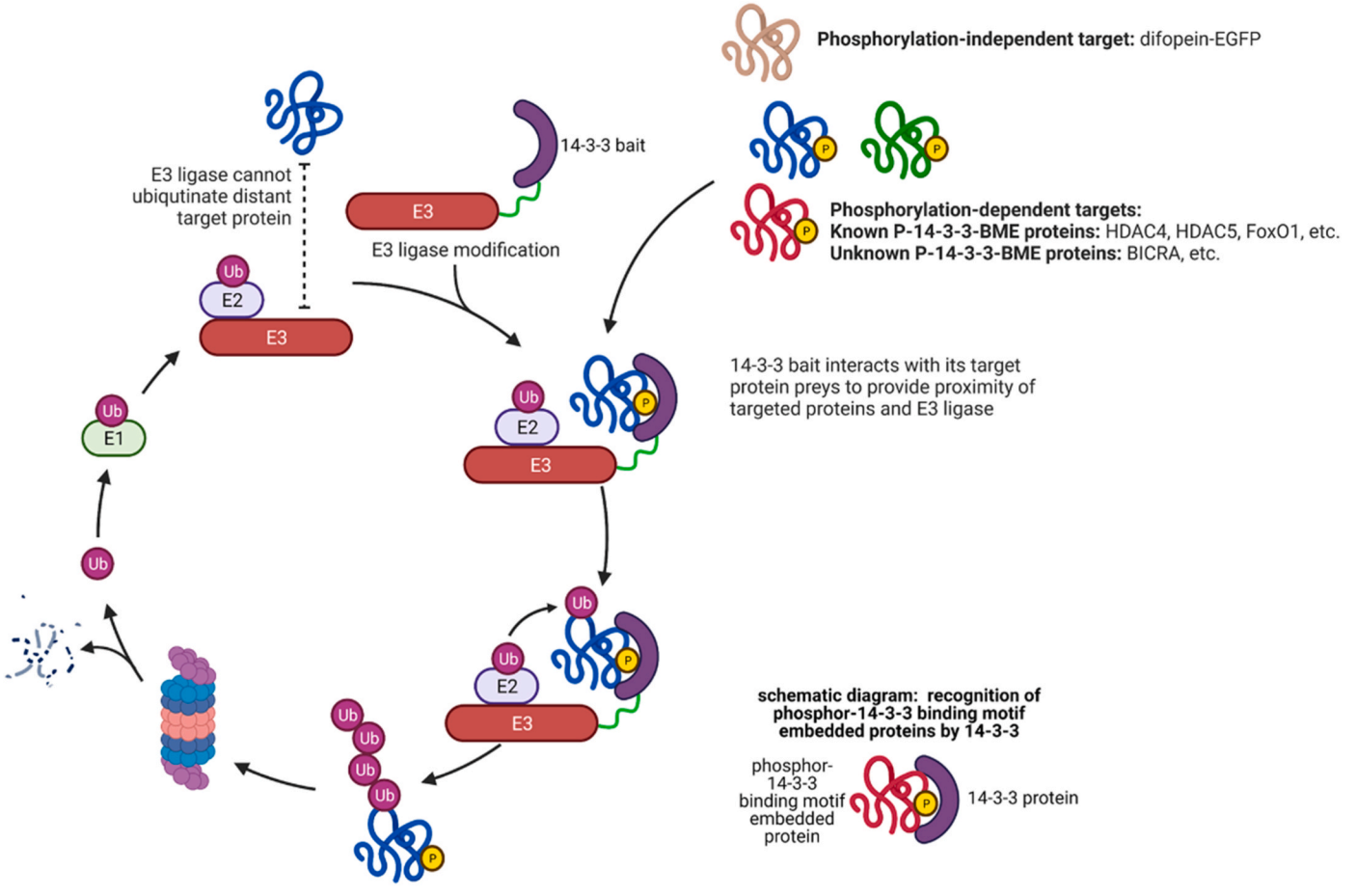

Fig. 5. Working model of TDPP, a ubiquitination-mediated degradation system to target 14-3-3-binding phosphoproteins.

Protein phosphorylation/dephosphorylation plays as a "switch" to activate or inactivate phosphatidylinositol 3-kinase [62]. A simple degradation of the total protein is unspecified and the degradation of proteins with or without PTMs cannot be told apart. PPIs are also affected by PTMs [63]. Proteins with PTMs can be recognized by their specific "readers", such as Forkhead-associated (FHA) domains for protein phosphorylation [64], and bromodomains for histone acetylation [65]. For 14-3-3-BPPs, three typical kinds of the binding motifs have been identified with high affinity to 14-3-3, the dominating RXX(pS/pT)XP (mode I), and two other modes, RXXXpSXP (mode II) and (pS/pT)$X_{0\text{-}2}$-COOH (mode III), where pS/pT represents phosphoserine/phosphothreonine [66,67]. For 14-3-3-BPPs evaluated in this study, the known and potential 14-3-3 binding motifs contained in those proteins can be grouped as mode I and II, and there is no difference between successfully degraded and undegraded proteins in 14-3-3-binding motif modes. Thus, based on the design and our results, it is presumed that TDPP could have great degradation efficiency for proteins with those three kinds of motifs, and the difference in degradation efficiency should be attributed to unfavorable interacting conditions discussed above but not the interaction ability. While 14-3-3 and 14-3-3-BPPs are involved in many cellular events, including neural development [68], cancer proliferation and apoptosis [69–71], autoimmune disorder [72], virus infection [73], etc., the TDPP-induced degradation could be significant in regulating the related downstream pathways and biological events.

The strategy of designing TDPP is scalable and it can be easily extended to target other proteins that share similar characteristics. For example, H3K9ac-embedded histones may be targeted by bromodomain-embedded proteins ligated with E3-ligases. We are enthusiastic that the design of TDPP will inspire more targeted degradation designs, especially those targeting a specific interactome, and thus inspiring more ideas in the designing of TPD systems.

In summary, we describe a TPD strategy, the TDPP system, that specifically targets and degrades 14-3-3-BPPs. We have validated the degradation efficiency and mechanism of TDPP with a difopein-EGFP system, and general and specific 14-3-3-BPPs. As the first phosphorylation-induced TPD system, TDPP not only can inspire more similar strategies in TPD designing, but also could be a powerful tool to regulate phospho-14-3-3 binding motif levels and validate unidentified 14-3-3 binding proteins, which are very important to 14-3-3 related research.

3.1. Limitations of the study

The major concern about TDPP is its targeting specificity. Certain potential mechanisms may make TDPP-induced degradation off-target. In theory, some non-14-3-3-BPPs may be degraded by TDPP through nonspecific binding to 14-3-3 (i.e., not bind to the binding groove of 14-3-3). Specifically, one scenario that we should pay more attention to is the 14-3-3 dimerization [74], where the heterodimerization of TDPP and an endogenous 14-3-3 protein could potentially deplete 14-3-3 in cells. Another case is condensates existing in cells [75]; some proteins may condense to a specific cellular location and have specific functions. Such a condensate behavior, however, may lead TDPP to target a protein without a phospho-14-3-3 binding motif. Therefore, TDPP as a prototype for phosphorylation-based degradation system will need to be customized for further specific application.

Another potential weakness of this study is that only one kind of phosphorylated forms of HDAC4, HDAC4 pS632 was selected in the single-protein evaluation that TDPP is a phosphorylation-dependent TPD system. However, the results of phospho-(Ser)-14-3-3-binding-motif (Fig. 3, A-C) have clearly proved the phosphorylation-dependent degradation mechanism described here in a multiple-protein manner. While more antibodies are available, which targeting suitable phosphoproteins, further evaluation could be performed.

4. Methods

4.1. Key resources table

The key resources table can be found in Supplement File 1.

4.2. Resource availability

4.2.1. Lead contact

Further information and requests for resources and reagents should be directed to and will be fulfilled by the lead contact, Liu Liu (luvul@med.umich.edu).

4.2.2. Materials availability

The materials underlying this article will be shared upon reasonable request to the lead contact, Liu Liu.

4.2.3. Data and code availability

Data generated in this study are provided in the article and its associated files. Source data are provided with this paper. All other data will be shared by the lead contact upon request.

This paper did not generate code.

Any additional information required to reanalyze the data reported in this paper is available from the lead contact upon request.

4.3. Experimental model and subject details

4.3.1. Mammalian cells and cell culture

HEK 293T/17 cells were cultured according to ATCC's protocol with minor optimizations. For a typical cell culture cycle with transfection, cells were seeded at 50×10^3 cells/cm^2 density, and 24 h (hrs) after cell seeding, attached cells were transfected with plasmid or plasmids mix encoded with desired gene(s) with Lipofectamine 2000 following manufacture's protocol. 48 hrs after transfection, cells were collected for further evaluations.

4.4. Method details

4.4.1. Plasmid information

Plasmids encoded with VHL, 14-3-3ζ, HDAC4, HDAC5, FoxO1, CFL1, BICRA were obtained from Addgene. Difopein DNA was constructed with 3 ssDNA oligos and 3 primers (sequence can be found in Table S1) by overlapping PCR. Plasmids encoded with VHL 3 KR-14-3-3ζ (1–230) 20 KR mutation, VHL 3 KR-14-3-3ζ (1–230) 19 KR K49E mutation were synthesized by GenScript Biotech. The transfection vectors of each gene described above were constructed into pcDNA3.1 backbone using PCR amplification.

4.4.2. Transfection

Transfection of HEK293T/17 cells was performed using Lipofectamine 2000 according to manufacturer's protocol.

4.4.3. Western blotting

Adherent cells were washed with pre-cooled Hank's balanced salt solution supplemented with phosphatase inhibitors and protease inhibitor cocktail. Cell pellets or protein supernatants were lysed in 1x Laemmli sample buffer containing beta-mercaptoethanol, phosphatase inhibitors and protease inhibitor cocktail. The whole-cell lysates were normalized to same protein concentration and then separated using SDS-PAGE, sequenced by transferring onto polyvinyllidene difluoride membranes. The membrane was incubated with a blocking solution consisting of 3% bovine serum albumin (BSA) in TBS solution for phosphorylated proteins of interest, or 4% non-fat dry milk (NFDM) in PBS solution for other proteins of interest. The membrane was blocked for 3 times and 10 min each time at room temperature, then incubated with primary antibodies in blocking solution overnight at 4 °C, followed by incubation with host-specific Alexa Fluor-conjugated secondary antibodies (1:10000 dilution) for 1 h. For signal detection, the membrane was developed directly with a LI-COR Imaging System. The developed bands were analyzed with Image Studio (LI-COR) or ImageJ (NIH) software. All unedited full-length gel images could be found in Supplement File 2.

4.4.4. Co-immunoprecipitation

The co-immunoprecipitation method was performed to investigate protein-protein interactions. HEK293T/17 cells were transfected with indicated constructs as described in "Transfection" section. Adherent cells were washed with cold HBSS supplemented with phosphatase inhibitors and protease inhibitor cocktail, sequenced by cells scraping and lysing the cell pellets in immunoprecipitation lysis buffer (150 mM NaCl, 1% Triton X-100 in 20 mM HEPES, supplemented with phosphatase inhibitors and protease inhibitor cocktail) for 30 min on rotator at 4 °C. Next, the supernatant was separated by centrifuging at 13,000 g at 4 °C for 5 min and collected, to which the normal mouse IgG, normal rabbit IgG, or antibodies against protein of interest, and Protein G Dyna beads were supplemented and incubated with the cell lysate at 4 °C on a rotor overnight. The beads were washed four times with IP buffer (150 mM NaCl, 0.05% TWEENS 20 in 20 mM HEPES, supplemented with phosphatase inhibitors and protease inhibitor cocktail), resuspended in 1x Laemmli Sample Buffer containing beta-mercaptoethanol, phosphatase inhibitors and protease inhibitor cocktail, followed by SDS-PAGE and immunoblotting with specified antibodies.

4.4.5. Fluorescence assay

HEK293T/17 cells were transfected with indicated constructs as described in "Transfection" section. For difopein-EGFP transfected HEK293T/17 cells, the nuclei were stained with Hoechst 33342 for 1 h prior the fluorescence assay, and EGFP fluorescence assay was performed under an inverted fluorescence microscope (Olympus IX73P2F), followed by image analysis with ImageJ software. For each microscope field, the fluorescence intensity under green and blue channel were considered as representative of EGFP intensity and cell number, respectively. The EGFP intensity was then normalized for each field by dividing intensity of green channel with intensity of blue channel.

4.5. Quantification and statistical analysis

4.5.1. Statistical analysis

Results were presented as mean ± SEM. Statistically significant differences between groups were analyzed by two-tailed, unpaired Student's t-test or one-way analysis of variance (ANOVA) followed by the Student-Newman-Keuls multiple comparisons tests using Prism 8 software. A p-value <0.05 was regarded as significant. Each experiment was performed at least three times.

Author contribution statement

Zhaokai Li, Liu Liu: Conceived and designed the experiments; Performed the experiments; Analyzed and interpreted the data;

Contributed reagents, materials, analysis tools or data; Wrote the paper.

Xiaoqiang Huang, Mohan Li: Analyzed and interpreted the data; Contributed reagents, materials, analysis tools or data; Wrote the paper.

Y. Eugene Chen, Zhong Wang: Conceived and designed the experiments; Contributed reagents, materials, analysis tools or data; Wrote the paper.

Funding statement

Zhong Wang was supported by National Institutes of Health {R01HL139735; R01HL163672}

Data availability statement

Data included in article/supplementary material/referenced in article.

Declaration of competing interest

The authors declare that they have no known competing financial interests or personal relationships that could have appeared to influence the work reported in this paper.

Acknowledgements

This research was supported in part by R01HL139735 and R01HL163672 to ZW. We would like to thank Dr. Shaomeng Wang for suggestions, Dr. Leonid Bnatovskiy and Ziad Sabry for editing the manuscript.

Fig. 1A, B, 2A and 5 were created with BioRender.com.

Appendix A. Supplementary data

Supplementary data to this article can be found online at https://doi.org/10.1016/j.heliyon.2023.e16318.

References

[1] Y. Ding, Y. Fei, B. Lu, Emerging new concepts of degrader technologies, Trends Pharmacol. Sci. 41 (2020) 464–474, https://doi.org/10.1016/j.tips.2020.04.005.
[2] C.M. Pickart, Mechanisms underlying ubiquitination, Annu. Rev. Biochem. 70 (2001) 503–533, https://doi.org/10.1146/annurev.biochem.70.1.503.
[3] N. Zheng, N. Shabek, Ubiquitin ligases: structure, function, and regulation, Annu. Rev. Biochem. 86 (2017) 129–157, https://doi.org/10.1146/annurev-biochem-060815-014922.
[4] A.R. Schneekloth, M. Pucheault, H.S. Tae, C.M. Crews, Targeted intracellular protein degradation induced by a small molecule: en route to chemical proteomics, Bioorg. Med. Chem. Lett 18 (2008) 5904–5908, https://doi.org/10.1016/j.bmcl.2008.07.114.
[5] L.J. Fulcher, T. Macartney, P. Bozatzi, A. Hornberger, A. Rojas-Fernandez, G.P. Sapkota, An affinity-directed protein missile system for targeted proteolysis, Open Biol 6 (2016), 160255, https://doi.org/10.1098/rsob.160255.
[6] X. Tan, L.I. Calderon-Villalobos, M. Sharon, C. Zheng, C.V. Robinson, M. Estelle, N. Zheng, Mechanism of auxin perception by the TIR1 ubiquitin ligase, Nature 446 (2007) 640–645, https://doi.org/10.1038/nature05731.
[7] B. Nabet, J.M. Roberts, D.L. Buckley, J. Paulk, S. Dastjerdi, A. Yang, A.L. Leggett, M.A. Erb, M.A. Lawlor, A. Souza, et al., The dTAG system for immediate and target-specific protein degradation, Nat. Chem. Biol. 14 (2018) 431–441, https://doi.org/10.1038/s41589-018-0021-8.
[8] T.K. Neklesa, H.S. Tae, A.R. Schneekloth, M.J. Stulberg, T.W. Corson, T.B. Sundberg, K. Raina, S.A. Holley, C.M. Crews, Small-molecule hydrophobic tagging-induced degradation of HaloTag fusion proteins, Nat. Chem. Biol. 7 (2011) 538–543, https://doi.org/10.1038/nchembio.597.
[9] D.L. Buckley, K. Raina, N. Darricarrere, J. Hines, J.L. Gustafson, I.E. Smith, A.H. Miah, J.D. Harling, C.M. Crews, HaloPROTACS: use of small molecule PROTACs to induce degradation of HaloTag fusion proteins, ACS Chem. Biol. 10 (2015) 1831–1837, https://doi.org/10.1021/acschembio.5b00442.
[10] G.M. Burslem, C.M. Crews, Proteolysis-targeting chimeras as therapeutics and tools for biological discovery, Cell 181 (2020) 102–114, https://doi.org/10.1016/j.cell.2019.11.031.
[11] K. Sharma, Rochelle C.J. D'Souza, S. Tyanova, C. Schaab, Jacek R. Wiśniewski, J. Cox, M. Mann, Ultradeep human phosphoproteome reveals a distinct regulatory nature of tyr and ser/thr-based signaling, Cell Rep. 8 (2014) 1583–1594, https://doi.org/10.1016/j.celrep.2014.07.036.
[12] F. Ardito, M. Giuliani, D. Perrone, G. Troiano, L. Lo Muzio, The crucial role of protein phosphorylation in cell signaling and its use as targeted therapy (Review), Int. J. Mol. Med. 40 (2017) 271–280, https://doi.org/10.3892/ijmm.2017.3036.
[13] M. Wang, C.J. Herrmann, M. Simonovic, D. Szklarczyk, C. von Mering, Version 4.0 of PaxDb: protein abundance data, integrated across model organisms, tissues, and cell-lines, Proteomics 15 (2015) 3163–3168, https://doi.org/10.1002/pmic.201400441.
[14] B. Cornell, K. Toyo-Oka, 14-3-3 proteins in brain development: neurogenesis, neuronal migration and neuromorphogenesis, Front. Mol. Neurosci. 10 (2017) 318, https://doi.org/10.3389/fnmol.2017.00318.
[15] H. Fu, R.R. Subramanian, S.C. Masters, 14-3-3 proteins: structure, function, and regulation, Annu. Rev. Pharmacol. Toxicol. 40 (2000) 617–647, https://doi.org/10.1146/annurev.pharmtox.40.1.617.
[16] C.J. Diehl, A. Ciulli, Discovery of small molecule ligands for the von Hippel-Lindau (VHL) E3 ligase and their use as inhibitors and PROTAC degraders, Chem. Soc. Rev. 51 (2022) 8216–8257, https://doi.org/10.1039/d2cs00387b.
[17] A.P. Crew, K. Raina, H. Dong, Y. Qian, J. Wang, D. Vigil, Y.V. Serebrenik, B.D. Hamman, A. Morgan, C. Ferraro, et al., Identification and characterization of von hippel-lindau-recruiting proteolysis targeting chimeras (PROTACs) of TANK-binding kinase 1, J. Med. Chem. 61 (2018) 583–598, https://doi.org/10.1021/acs.jmedchem.7b00635.
[18] E. Caussinus, O. Kanca, M. Affolter, Fluorescent fusion protein knockout mediated by anti-GFP nanobody, Nat. Struct. Mol. Biol. 19 (2011) 117–121, https://doi.org/10.1038/nsmb.2180.

[19] A.F.M. Ibrahim, L. Shen, M.H. Tatham, D. Dickerson, A.R. Prescott, N. Abidi, D.P. Xirodimas, R.T. Hay, Antibody RING-mediated destruction of endogenous proteins, Mol. Cell 79 (2020) 155–166, https://doi.org/10.1016/j.molcel.2020.04.032.

[20] L.J. Fulcher, L.D. Hutchinson, T.J. Macartney, C. Turnbull, G.P. Sapkota, Targeting endogenous proteins for degradation through the affinity-directed protein missile system, Open Biol 7 (2017), https://doi.org/10.1098/rsob.170066.

[21] V. Zoppi, S.J. Hughes, C. Maniaci, A. Testa, T. Gmaschitz, C. Wieshofer, M. Koegl, K.M. Riching, D.L. Daniels, A. Spallarossa, A. Ciulli, Iterative design and optimization of initially inactive proteolysis targeting chimeras (PROTACs) identify VZ185 as a potent, fast, and selective von Hippel-lindau (VHL) based dual degrader probe of BRD9 and BRD7, J. Med. Chem. 62 (2019) 699–726, https://doi.org/10.1021/acs.jmedchem.8b01413.

[22] A.B. Truong, S.C. Masters, H. Yang, H. Fu, Role of the 14-3-3 C-terminal loop in ligand interaction, Proteins 49 (2002) 321–325, https://doi.org/10.1002/prot.10210.

[23] V. Obsilova, P. Herman, J. Vecer, M. Sulc, J. Teisinger, T. Obsil, 14-3-3zeta C-terminal stretch changes its conformation upon ligand binding and phosphorylation at Thr232, J. Biol. Chem. 279 (2004) 4531–4540, https://doi.org/10.1074/jbc.M306939200.

[24] J. Silhan, V. Obsilova, J. Vecer, P. Herman, M. Sulc, J. Teisinger, T. Obsil, 14-3-3 protein C-terminal stretch occupies ligand binding groove and is displaced by phosphopeptide binding, J. Biol. Chem. 279 (2004) 49113–49119, https://doi.org/10.1074/jbc.M408671200.

[25] Q. Yin, T. Han, B. Fang, G. Zhang, C. Zhang, E.R. Roberts, V. Izumi, M. Zheng, S. Jiang, X. Yin, et al., K27-linked ubiquitination of BRAF by ITCH engages cytokine response to maintain MEK-ERK signaling, Nat. Commun. 10 (2019) 1870, https://doi.org/10.1038/s41467-019-09844-0.

[26] M. Mirdita, K. Schutze, Y. Moriwaki, L. Heo, S. Ovchinnikov, M. Steinegger, ColabFold: making protein folding accessible to all, Nat. Methods 19 (2022) 679–682, https://doi.org/10.1038/s41592-022-01488-1.

[27] J. Jumper, R. Evans, A. Pritzel, T. Green, M. Figurnov, O. Ronneberger, K. Tunyasuvunakool, R. Bates, A. Zidek, A. Potapenko, et al., Highly accurate protein structure prediction with AlphaFold, Nature 596 (2021) 583–589, https://doi.org/10.1038/s41586-021-03819-2.

[28] V. Mariani, M. Biasini, A. Barbato, T. Schwede, lDDT: a local superposition-free score for comparing protein structures and models using distance difference tests, Bioinformatics 29 (2013) 2722–2728, https://doi.org/10.1093/bioinformatics/btt473.

[29] B. Wang, H. Yang, Y.C. Liu, T. Jelinek, L. Zhang, E. Ruoslahti, H. Fu, Isolation of high-affinity peptide antagonists of 14-3-3 proteins by phage display, Biochemistry 38 (1999) 12499–12504, https://doi.org/10.1021/bi991353h.

[30] S.C. Masters, H. Fu, 14-3-3 proteins mediate an essential anti-apoptotic signal, J. Biol. Chem. 276 (2001) 45193–45200, https://doi.org/10.1074/jbc.M105971200.

[31] L. Zhang, H. Wang, D. Liu, R. Liddington, H. Fu, Raf-1 kinase and exoenzyme S interact with 14-3-3zeta through a common site involving lysine 49, J. Biol. Chem. 272 (1997) 13717–13724, https://doi.org/10.1074/jbc.272.21.13717.

[32] E.M. Ramser, G. Wolters, G. Dityateva, A. Dityatev, M. Schachner, T. Tilling, The 14-3-3zeta protein binds to the cell adhesion molecule L1, promotes L1 phosphorylation by CKII and influences L1-dependent neurite outgrowth, PLoS One 5 (2010), e13462, https://doi.org/10.1371/journal.pone.0013462.

[33] L.M. Cockrell, M.C. Puckett, E.H. Goldman, F.R. Khuri, H. Fu, Dual engagement of 14-3-3 proteins controls signal relay from ASK2 to the ASK1 signalosome, Oncogene 29 (2010) 822–830, https://doi.org/10.1038/onc.2009.382.

[34] K. Nishimura, T. Fukagawa, H. Takisawa, T. Kakimoto, M. Kanemaki, An auxin-based degron system for the rapid depletion of proteins in nonplant cells, Nat. Methods 6 (2009) 917–922, https://doi.org/10.1038/nmeth.1401.

[35] D. Clift, W.A. McEwan, L.I. Labzin, V. Konieczny, B. Mogessie, L.C. James, M. Schuh, A method for the acute and rapid degradation of endogenous proteins, Cell 171 (2017) 1692–1706 e1618, https://doi.org/10.1016/j.cell.2017.10.033.

[36] A.B. Dounay, C.J. Forsyth, Okadaic acid: the archetypal serine/threonine protein phosphatase inhibitor, Curr. Med. Chem. 9 (2002) 1939–1980, https://doi.org/10.2174/0929867023368791.

[37] Z. Wang, G. Qin, T.C. Zhao, HDAC4: mechanism of regulation and biological functions, Epigenomics 6 (2014) 139–150, https://doi.org/10.2217/epi.13.73.

[38] T.A. McKinsey, C.L. Zhang, J. Lu, E.N. Olson, Signal-dependent nuclear export of a histone deacetylase regulates muscle differentiation, Nature 408 (2000) 106–111, https://doi.org/10.1038/35040593.

[39] J. Yang, C. Gong, Q. Ke, Z. Fang, X. Chen, M. Ye, X. Xu, Insights into the function and clinical application of HDAC5 in cancer management, Front. Oncol. 11 (2021), 661620, https://doi.org/10.3389/fonc.2021.661620.

[40] Z. Cheng, FoxO transcription factors in mitochondrial homeostasis, Biochem. J. 479 (2022) 525–536, https://doi.org/10.1042/BCJ20210777.

[41] P. Hotulainen, E. Paunola, M.K. Vartiainen, P. Lappalainen, Actin-depolymerizing factor and cofilin-1 play overlapping roles in promoting rapid F-actin depolymerization in mammalian nonmuscle cells, Mol. Biol. Cell 16 (2005) 649–664, https://doi.org/10.1091/mbc.e04-07-0555.

[42] G. Kanellos, M.C. Frame, Cellular functions of the ADF/cofilin family at a glance, J. Cell Sci. 129 (2016) 3211–3218, https://doi.org/10.1242/jcs.187849.

[43] A.H. Wang, M.J. Kruhlak, J. Wu, N.R. Bertos, M. Vezmar, B.I. Posner, D.P. Bazett-Jones, X.J. Yang, Regulation of histone deacetylase 4 by binding of 14-3-3 proteins, Mol. Cell Biol. 20 (2000) 6904–6912, https://doi.org/10.1128/MCB.20.18.6904-6912.2000.

[44] C.M. Grozinger, S.L. Schreiber, Regulation of histone deacetylase 4 and 5 and transcriptional activity by 14-3-3-dependent cellular localization, Proc. Natl. Acad. Sci. U. S. A. 97 (2000) 7835–7840, https://doi.org/10.1073/pnas.140199597.

[45] X. Zhao, A. Ito, C.D. Kane, T.S. Liao, T.A. Bolger, S.M. Lemrow, A.R. Means, T.P. Yao, The modular nature of histone deacetylase HDAC4 confers phosphorylation-dependent intracellular trafficking, J. Biol. Chem. 276 (2001) 35042–35048, https://doi.org/10.1074/jbc.M105086200.

[46] T.G. Nishino, M. Miyazaki, H. Hoshino, Y. Miwa, S. Horinouchi, M. Yoshida, 14-3-3 regulates the nuclear import of class IIa histone deacetylases, Biochem. Biophys. Res. Commun. 377 (2008) 852–856, https://doi.org/10.1016/j.bbrc.2008.10.079.

[47] G. Paroni, N. Cernotta, C. Dello Russo, P. Gallinari, M. Pallaoro, C. Foti, F. Talamo, L. Orsatti, C. Steinkuhler, C. Brancolini, PP2A regulates HDAC4 nuclear import, Mol. Biol. Cell 19 (2008) 655–667, https://doi.org/10.1091/mbc.e07-06-0623.

[48] Y. Kondo, J. Ognjenovic, S. Banerjee, D. Karandur, A. Merk, K. Kulhanek, K. Wong, J.P. Roose, S. Subramaniam, J. Kuriyan, Cryo-EM structure of a dimeric B-Raf:14-3-3 complex reveals asymmetry in the active sites of B-Raf kinases, Science 366 (2019) 109–115, https://doi.org/10.1126/science.aay0543.

[49] Z. Wang, W. Zhai, J.A. Richardson, E.N. Olson, J.J. Meneses, M.T. Firpo, C. Kang, W.C. Skarnes, R. Tjian, Polybromo protein BAF180 functions in mammalian cardiac chamber maturation, Genes Dev. 18 (2004) 3106–3116, https://doi.org/10.1101/gad.1238104.

[50] X. Gao, P. Tate, P. Hu, R. Tjian, W.C. Skarnes, Z. Wang, ES cell pluripotency and germ-layer formation require the SWI/SNF chromatin remodeling component BAF250a, Proc. Natl. Acad. Sci. U. S. A. 105 (2008) 6656–6661, https://doi.org/10.1073/pnas.0801802105.

[51] I. Lei, L. Liu, M.H. Sham, Z. Wang, SWI/SNF in cardiac progenitor cell differentiation, J. Cell. Biochem. 114 (2013) 2437–2445, https://doi.org/10.1002/jcb.24570.

[52] I. Lei, J. West, Z. Yan, X. Gao, P. Fang, J.H. Dennis, L. Gnatovskiy, W. Wang, R.E. Kingston, Z. Wang, BAF250a protein regulates nucleosome occupancy and histone modifications in priming embryonic stem cell differentiation, J. Biol. Chem. 290 (2015) 19343–19352, https://doi.org/10.1074/jbc.M115.637389.

[53] I. Lei, S. Tian, V. Chen, Y. Zhao, Z. Wang, SWI/SNF component BAF250a coordinates OCT4 and WNT signaling pathway to control cardiac lineage differentiation, Front. Cell Dev. Biol. 7 (2019) 358, https://doi.org/10.3389/fcell.2019.00358.

[54] P.K. Parua, K.M. Dombek, E.T. Young, Yeast 14-3-3 protein functions as a comodulator of transcription by inhibiting coactivator functions, J. Biol. Chem. 289 (2014) 35542–35560, https://doi.org/10.1074/jbc.M114.592287.

[55] F. Madeira, M. Tinti, G. Murugesan, E. Berrett, M. Stafford, R. Toth, C. Cole, C. MacKintosh, G.J. Barton, 14-3-3-Pred: improved methods to predict 14-3-3-binding phosphopeptides, Bioinformatics 31 (2015) 2276–2283, https://doi.org/10.1093/bioinformatics/btv133.

[56] S. Barish, T.S. Barakat, B.C. Michel, N. Mashtalir, J.B. Phillips, A.M. Valencia, B. Ugur, J. Wegner, T.M. Scott, B. Bostwick, et al., BICRA, a SWI/SNF complex member, is associated with BAF-disorder related phenotypes in humans and model organisms, Am. J. Hum. Genet. 107 (2020) 1096–1112, https://doi.org/10.1016/j.ajhg.2020.11.003.

[57] J.B. Mortenson, L.N. Heppler, C.J. Banks, V.K. Weerasekara, M.D. Whited, S.R. Piccolo, W.E. Johnson, J.W. Thompson, J.L. Andersen, Histone deacetylase 6 (HDAC6) promotes the pro-survival activity of 14-3-3zeta via deacetylation of lysines within the 14-3-3zeta binding pocket, J. Biol. Chem. 290 (2015) 12487–12496, https://doi.org/10.1074/jbc.M114.607580.

[58] K.L. Pennington, T.Y. Chan, M.P. Torres, J.L. Andersen, The dynamic and stress-adaptive signaling hub of 14-3-3: emerging mechanisms of regulation and context-dependent protein-protein interactions, Oncogene 37 (2018) 5587–5604, https://doi.org/10.1038/s41388-018-0348-3.
[59] C. Choudhary, C. Kumar, F. Gnad, M.L. Nielsen, M. Rehman, T.C. Walther, J.V. Olsen, M. Mann, Lysine acetylation targets protein complexes and co-regulates major cellular functions, Science 325 (2009) 834–840, https://doi.org/10.1126/science.1175371.
[60] G. Gogl, K.V. Tugaeva, P. Eberling, C. Kostmann, G. Trave, N.N. Sluchanko, Hierarchized phosphotarget binding by the seven human 14-3-3 isoforms, Nat. Commun. 12 (2021) 1677, https://doi.org/10.1038/s41467-021-21908-8.
[61] K.V. Tugaeva, D. Hawkins, J.L.R. Smith, O.W. Bayfield, D.S. Ker, A.A. Sysoev, O.I. Klychnikov, A.A. Antson, N.N. Sluchanko, The mechanism of SARS-CoV-2 nucleocapsid protein recognition by the human 14-3-3 proteins, J. Mol. Biol. 433 (2021), 166875, https://doi.org/10.1016/j.jmb.2021.166875.
[62] B.A. Hemmings, D.F. Restuccia, PI3K-PKB/Akt pathway, Cold Spring Harbor Perspect. Biol. 4 (2012) a011189, https://doi.org/10.1101/cshperspect.a011189.
[63] O. Keskin, N. Tuncbag, A. Gursoy, Predicting protein-protein interactions from the molecular to the proteome level, Chem. Rev. 116 (2016) 4884–4909, https://doi.org/10.1021/acs.chemrev.5b00683.
[64] A.W. Almawi, L.A. Matthews, A. Guarne, FHA domains: phosphopeptide binding and beyond, Prog. Biophys. Mol. Biol. 127 (2017) 105–110, https://doi.org/10.1016/j.pbiomolbio.2016.12.003.
[65] T. Fujisawa, P. Filippakopoulos, Functions of bromodomain-containing proteins and their roles in homeostasis and cancer, Nat. Rev. Mol. Cell Biol. 18 (2017) 246–262, https://doi.org/10.1038/nrm.2016.143.
[66] X. Yang, W.H. Lee, F. Sobott, E. Papagrigoriou, C.V. Robinson, J.G. Grossmann, M. Sundstrom, D.A. Doyle, J.M. Elkins, Structural basis for protein-protein interactions in the 14-3-3 protein family, Proc. Natl. Acad. Sci. U. S. A. 103 (2006) 17237–17242, https://doi.org/10.1073/pnas.0605779103.
[67] C. Johnson, S. Crowther, M.J. Stafford, D.G. Campbell, R. Toth, C. MacKintosh, Bioinformatic and experimental survey of 14-3-3-binding sites, Biochem. J. 427 (2010) 69–78, https://doi.org/10.1042/BJ20091834.
[68] A. Antunes, V.M. Saia-Cereda, F. Crunfli, D. Martins-de-Souza, 14-3-3 proteins at the crossroads of neurodevelopment and schizophrenia, World J. Biol. Psychiatr. 23 (2022) 14–32, https://doi.org/10.1080/15622975.2021.1925585.
[69] X. Yang, W. Cao, X. Wang, X. Zhang, W. Zhang, Z. Li, H. Fu, Down-regulation of 14-3-3zeta reduces proliferation and increases apoptosis in human glioblastoma, Cancer Gene Ther. 27 (2020) 399–411, https://doi.org/10.1038/s41417-019-0097-7.
[70] G. Aljabal, B.K. Yap, 14-3-3sigma and its modulators in cancer, Pharmaceuticals 13 (2020) 441, https://doi.org/10.3390/ph13120441.
[71] Y. Huang, M. Yang, W. Huang, 14-3-3 sigma: a potential biomolecule for cancer therapy, Clin. Chim. Acta 511 (2020) 50–58, https://doi.org/10.1016/j.cca.2020.09.009.
[72] J. McGowan, C. Peter, J. Kim, S. Popli, B. Veerman, J. Saul-McBeth, H. Conti, S.M. Pruett-Miller, S. Chattopadhyay, R. Chakravarti, 14-3-3zeta-TRAF5 axis governs interleukin-17A signaling, Proc. Natl. Acad. Sci. U. S. A. 117 (2020) 25008–25017, https://doi.org/10.1073/pnas.2008214117.
[73] J. Liu, S. Cao, G. Ding, B. Wang, Y. Li, Y. Zhao, Q. Shao, J. Feng, S. Liu, L. Qin, Y. Xiao, The role of 14-3-3 proteins in cell signalling pathways and virus infection, J. Cell Mol. Med. 25 (2021) 4173–4182, https://doi.org/10.1111/jcmm.16490.
[74] Y.H. Shen, J. Godlewski, A. Bronisz, J. Zhu, M.J. Comb, J. Avruch, G. Tzivion, Significance of 14-3-3 self-dimerization for phosphorylation-dependent target binding, Mol. Biol. Cell 14 (2003) 4721–4733, https://doi.org/10.1091/mbc.e02-12-0821.
[75] A.S. Lyon, W.B. Peeples, M.K. Rosen, A framework for understanding the functions of biomolecular condensates across scales, Nat. Rev. Mol. Cell Biol. 22 (2021) 215–235, https://doi.org/10.1038/s41580-020-00303-z.